

Photopolymerization of Clay/Polyurethane Nanocomposites Induced by Intercalated Initiator

Hailin Tan, Jun Nie

State Key Laboratory of Chemical Resource Engineering, College of Materials Science and Engineering, Beijing University of Chemical Technology, Beijing 100029, People's Republic of China

Received 4 December 2006; accepted 19 March 2007

DOI 10.1002/app.26878

Published online 30 July 2007 in Wiley InterScience (www.interscience.wiley.com).

ABSTRACT: An intercalated initiator was synthesized and used for preparation of clay/polyurethane nanocomposites by UV irradiation. Organoclays containing initiator groups were prepared by cationic exchange process which acted as both suitable intercalant and photoinitiator. These modified clays were then dispersed in the mixture of urethane acrylate and hexanediol diacrylate in different loading, then *situ* photopolymerized. Intercalated and exfoliated

nanocomposite structure were evidenced by both X-ray diffraction spectroscopy and Transmission Electron Microscope. Thermal properties and morphologies of the resultant nanocomposites were also investigated. © 2007 Wiley Periodicals, Inc. *J Appl Polym Sci* 106: 2656–2660, 2007

Key words: montmorillonite; nanocomposites; photopolymerization; reactive organoclay; urethane acrylate

INTRODUCTION

UV-curable technology found increasing applications in micro and consumer electronics industries due to its rapid cure, solvent free characteristics, application versatility, low energy requirements, and low temperature operation.^{1–3} Because of the advantages of UV curing, and the possibility of exceptional physical property enhancements, such as stiffness, gas barrier, flammability retardance, etc.,^{4–8} in past decade, a lot of research focused on the UV curing polymer–clay nanocomposites.^{9–15}

To improve the affinity of montmorillonite toward organic materials, much research focused on the modification of montmorillonite with ammonium surfactants with polymerizable groups such as acrylate^{11–13} to build the chemical bonding between organoclay and polymer matrix. After photopolymerization, the hardness, scratch resistance, thermal stability and conductivity, polymerization shrinkage, and the mechanical properties were elevated without sacrificing optical properties.^{14,15} Weimer et al.¹⁶ first reported preparation of PS/clay nanocomposite by *situ* living free radical polymerization using a silicate-anchored initiator. Nese et al.¹⁷ prepared clay/PMMA nanocomposites using intercalated phenacyl pyridinium salt photoinitiators. XRD and TEM showed that interlayer spacing had been only enlarged to 1.6 nm which

might be attributed to that the photolytic initiatable radical fragment could diffuse outside of interlayer, and the polymer could not well intercalated into montmorillonite. To get well intercalation and exfoliation, the critical is the ability to enhance intragallery polymerization rate catalytically to be comparable or greater than extragallery polymerization.¹⁸

2-hydroxy-2-methyl-1-phenylpropane-1-one (1173) was a kind of common photoinitiator, and often was used to photoinitiate the free-radical polymerization of nanocomposites,^{11–13,19} which could split into two radical fragments, and both of the radical fragments could initiate polymerization with high efficiency. The current approach is expected to introduce 1173 into the interlayer to render clay surfaces organophilic and possess greater thermal stability than their aliphatic counterparts.²⁰ On UV irradiation, the splitted radical fragments were immobilized into the intergallery, allowing polymer molecules to grow inside the clay galleries. Consequently, this would promote direct formation of exfoliated nanocomposite structure, which is a general target to achieve improved mechanical properties.

EXPERIMENTAL

Materials

Diisocyanatoluene (TDI), dimethylethanolamine (DEA), and Di-*n*-butyltin dilaurate (DBT) were purchased from Beijing Chemical Reagent Company (Beijing, China). CN 964 and 1,6-hexanediol diacrylate (HDDA) were donated by Sartomer Company (Guangzhou, China), and used without further purification. 2-

Correspondence to: J. Nie (niejun@mail.buct.edu.cn).

Contract grant sponsor: National Natural Science Foundation of China; contract grant number: 50473024.

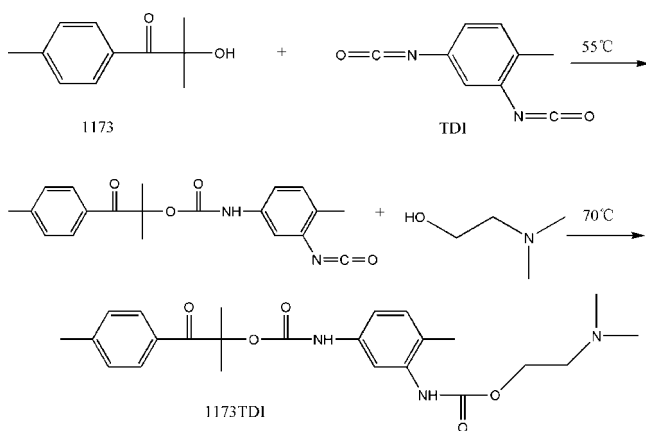


Figure 1 Synthesis of 1173TDI initiator.

hydroxy-2-methyl-1-phenylpropane-1-one (1173), was donated by Changzhou Runtec Chemical Co. (Changzhou, China). The silicate used was sodium montmorillonite (Na-MMT) from Liufangzi Clay Factory (Jilin, China), with a cationic exchange capacity (CEC) of 78 mequiv/100 g.

Synthesis of initiator amine (1173TDI)

A mixture of 8.7 g (0.05 mol) of TDI, 50 mL anhydrous ethyl acetate, and 0.2 g of DBT was added into a 250 mL three-necked flask equipped with stirrer, thermometer, and dropping funnel. Under oil bath about 55°C, 8.2 g (0.05 mol) of 1173 was added dropwise during 2 h. The mixture was allowed to stand 3 h, and FTIR indicated that the reaction finished after the disappearance O—H peaks at 3463 cm^{-1} , then the oil bath temperature was elevated to 70°C, and 4.46 g (0.05 mol) dimethylethanolamine (DEA) was added dropwise during 2 h. When FTIR showed the disappearance of NCO peaks at 2268 cm^{-1} , it indicated that all the reaction was finished. Subsequently, the solvent was removed on a rotary evaporator, and viscous liquid was obtained.

The yellow liquids were purified by silica gel (200–300 mesh) column chromatography using dichloromethane:ethanol = 4 : 1 (w/w) as an eluent, and slightly yellow product was obtained. The synthesis process and the structure of initiator 1173TDI were showed in Figure 1.

Preparation of organoclays

Modification of the Na-MMT

The clay mineral (1.5 g) was dispersed in 100 mL deionized water with magnetic stirrer for 2 h at 50°C, then 3 mL hydrochloride aqueous solution was added. Subsequently, 100 mL ethanolic solution of the initiator that corresponded to the CEC was added to the aqueous solution and stirred for about 5 h. The white sol formed was recovered by filtration, and

washed several times with deionized water and ethanol until no chloride was detected with 0.1N AgNO_3 solution. The modified clay was finally dried at 40°C for 24 h in vacuum. The product was ground with mortar, and sieved using a Cu griddle with 300 mesh. Organoclays were named 1173TDIMMT.

Dispersion of organo-clay in the photo-curing resins

The nanocomposite resin formulation was typically the following: the mixture of CN 964 (70 wt %) and HDDA (30 wt %) was employed as the photopolymerizable resin and varying concentrations of the organo-clay was used as the initiator and nanofiller. The organo-clay was dispersed into the UV-curable acrylic resin by first a stirring of the mixture, followed by a 8 h exposure in an ultrasound bath at 25°C, in the dark to prevent any premature polymerization.

Measurements

Series RTIR were recorded on a Nicolet 5700 instrument (Nicolet Instrument, ThermoCompany) to determine the conversion of double bond. The mixture of resin, organo-clay was placed in a mold made from glass slides and spacers with 15 ± 1 mm in diameter and 1.2 ± 0.1 mm in thickness. The light intensity on the surface of samples was detected by UV Light Radiometer (Beijing Normal University, China). The double bond conversion of the mixtures was monitored using near IR spectroscopy with the resolution of 4 cm^{-1} . The absorbance change of the =C—H peak area from 6100.70 to 6222.50 cm^{-1} was correlated to the extent of polymerization. The rate of polymerization could be calculated by the time derivative of the double bond conversion. For each sample, the series RTIR runs were repeated three times.

The XRD analyses were performed via X-ray diffractometer (Rigaku, Damax2500) with $\text{CuK}\alpha$ characteristic radiation (wavelength $\lambda = 0.154$ nm at 40 kV, 50 mA, and scan speed of 1°/min in the range of $2\theta = 0.5\text{--}10^\circ$).

Transmission electron micrographs were obtained on microtomed with a 45° diamond knife and mounted on 400 mesh copper grids. Bright-field transmission electron images were obtained on a Phillips CM200 transmission electron microscope at 200 kV.

Dynamic mechanical analysis (DMA) from -50 to $+150^\circ\text{C}$ with a ramping rate of 10°C/min was obtained in tensile rectangular mode of ~ 1.2 mm thickness and dimensions of 7×35 mm^2 on a Rheometrics DMTAV at 1 Hz and 0.005% strain.

Thermogravimetric data were obtained on a Mettler TG50 thermobalance equipped with a TC10A processor. A 7–10 mg sample was weighed and heated from 35 to 600°C at 10°C/min under a flow of 30 cm^3/min dry nitrogen carrier gas.

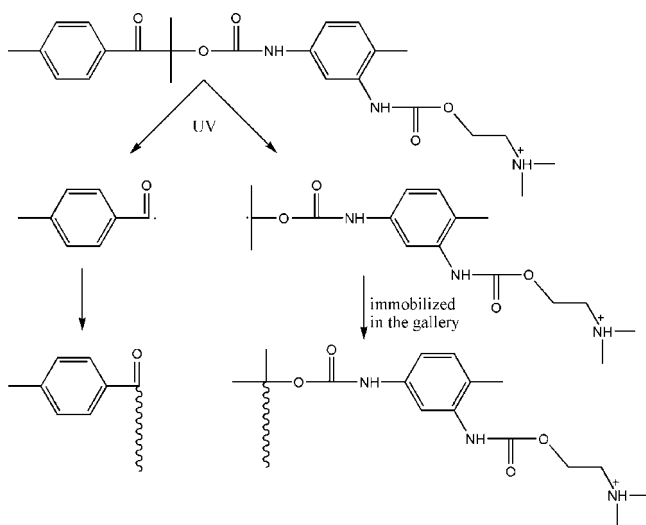


Figure 2 The photolytic process of 1173TDI on UV exposure.

For water sorption measurement, the samples were maintained at $(37 \pm 1)^\circ\text{C}$ for 24 h. The temperature was then decreased to 23°C for 1 h and the samples were subsequently weighed to an accuracy of ± 0.2 mg. This process was repeated until a constant mass m_1 was obtained. The specimen were then immersed in water and maintained at 37°C for several days. Every day the samples were taken out, washed with water, and weighed. This measurement was recorded as m_2 . Following this weighing, the specimens were replaced into water bath, and the cycle described previously was repeated until a final constant mass was obtained (m_2). For every polymer system, the value was average of five specimens. To calculate the water sorption (W_{sp}), the following equations were used:

$$W_{\text{sp}} = (m_2 - m_1) / m_1 \times 100\%$$

RESULTS AND DISCUSSION

The 1173TDI molecules were intercalated into the galleries of clays through cationic exchange. The excited 1173TDI underwent homolytic cleavage resulting in the formation of free radicals. Part of the free radicals could diffuse outside of layered silicate, and the other part of the free radicals were immobilized into the galleries, both of them were capable of initiating polymerization. The photoinitiated polymerization could be represented in Figure 2.

In these studies, the organoclay of varying concentration (1, 3, 5, 7/100) (w/w) was used as the photoinitiator. Under the irradiation of UV light, the polymerization of acrylate was initiated by the intercalated 1173TDI. Figure 3 graphically illustrated the double bond conversion versus UV light irradiation time of

resin mixture initiated by different concentration of organoclay exposed on 20 and 40 mW/cm^2 . It was obviously the concentration of montmorillonite had slightly some effect on the rate of photopolymerization and final double bond conversion.

The pure 1173 only 0.2/100 (w/w) had great reactivity toward the acrylate double bond, and high degree of conversion (close to 100%) could be reached after 10 s on UV exposure. The 1173TDIMMT system began to initiate polymerization after 100 s (20 mw) and 36 s (40 mw) on UV exposure. The higher concentration of the organoclay, the earlier the polymerization began. The stage that did not initiate the polymerization on UV exposure were called inducement stage. Though oxygen have inhibitory effect on photoinitiated radical polymerization, it could be conquered through increasing light intensity, sample thickness and excluding oxygen. In this study, oxygen inhibitory effect were conquered through increasing sample thickness (1.2 mm), and photopolymerization in a mold between two pieces of glass, so the inducement stage could be attributed to the diffusibility of photolysis radical fragments from intergallery to the resin ma-

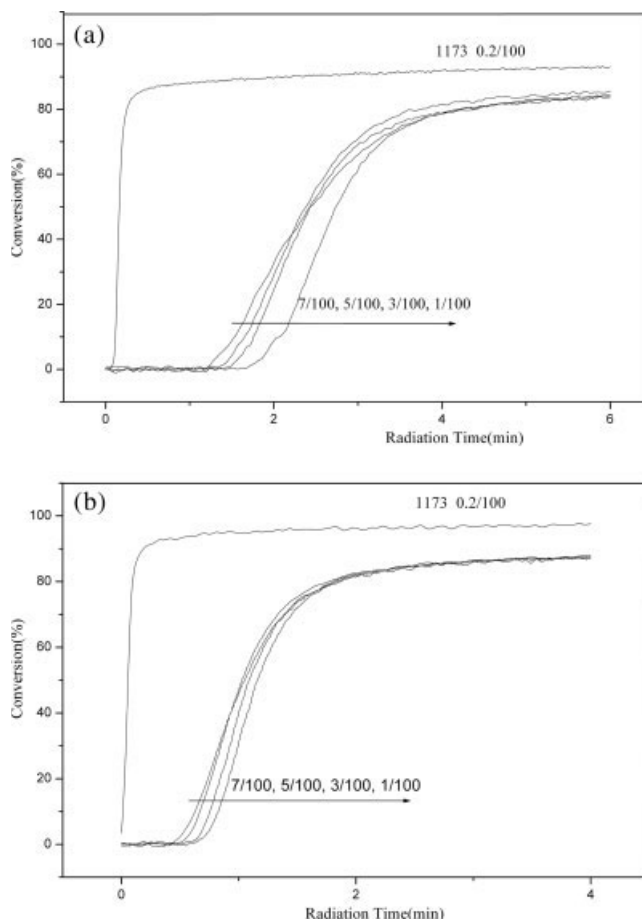


Figure 3 Double bond conversion versus irradiation time with different concentrations of the modified clay (w/w). (a) 20 mW/cm^2 (b) 40 mW/cm^2 .

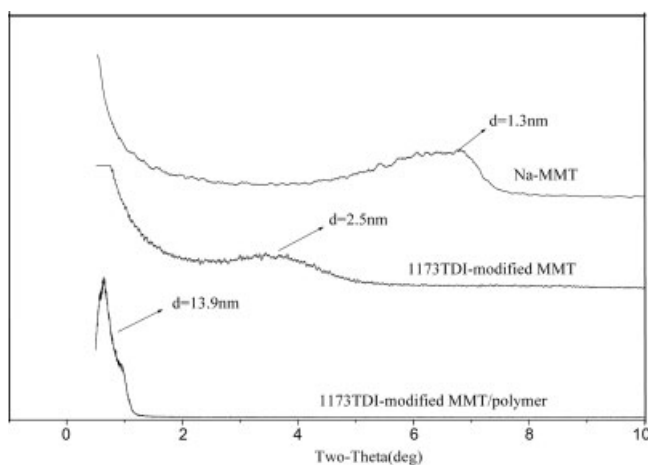


Figure 4 X-ray diffraction curves of Na-MMT, 1173TDIMMT and the composites with 5/100 (w/w) 1173TDIMMT loading.

trix, the photolysis radical fragments immobilized in the intergallery could only initiate polymerization in the gallery because it was very difficult for the resin to diffuse into the gallery during the polymerization.

The X-ray diffraction (XRD) was used to identify intercalated structures and determine the interlayer spacing. In Figure 4 a broad diffraction peak around $2\theta = 6.71^\circ$ was displayed by natural montmorillonite, equaling a d spacing of 1.3 nm for the layered silicates in montmorillonite. For the 1173TDIMMT, a XRD peak at $2\theta = 3.56^\circ$ resulted from the diffraction of the (0 0 1) crystal surface of layered silicates, indicating that layered silicates have been intercalated by 1173TDI molecules to a d spacing of 2.5 nm. When the organoclay was dispersed in the resin with 5/100 (w/w) loading and UV-cured, a strong diffraction peaks at $2\theta = 0.63^\circ$ was detected, corresponding to a d spacing of 13.9 nm, which indicated that the polymer intercalated into the layered silicate and enlarged the d spacing.

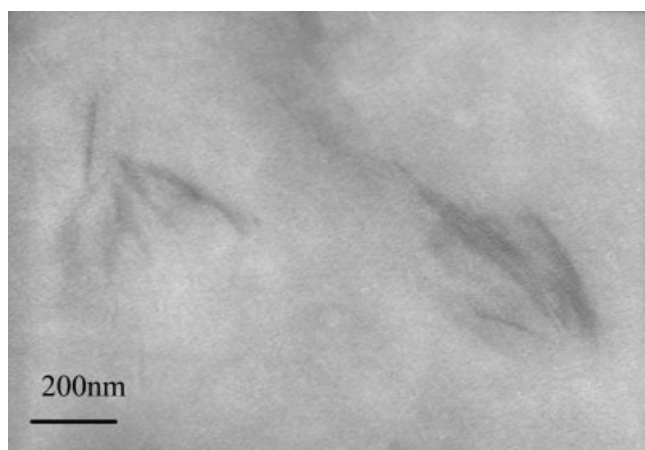


Figure 5 TEM micrograph of organoclay/polyurethane nanocomposites containing 5/100 (w/w) 1173TDIMMT.

To further investigate the nanocomposite structure and to confirm XRD results, transmission electron microscopy (TEM) was performed on the organoclay/polyurethane nanocomposite containing 5/100 (w/w) organoclay. Micrographs are illustrated in Figure 5. The clay platelets in the nanocomposites showed a parallel orientation. This was direct evidence that these silicate layers had been intercalated resin and a nanocomposite of partially exfoliated silicate layers and polyurethane resin had formed.

The viscoelastic characteristics of the nanocomposite photopolymers were measured by dynamic mechanical analysis (DMA) on 1.2 mm thick samples. Figure 6 shows the typical profiles recorded by DMA for a UV-cured polyurethane-acrylate by monitoring the variation of the storage modulus (E') and the tensile loss factor ($\tan \delta$) with increasing temperature. The addition of the layered silicate (5/100) causes a rise of the glass transition temperature (79°C vs. 67°C) and a small increase of the storage modulus. The increment in T_g of organoclay/polyurethane nanocomposite could be ascribed to its exfoliation morphology with fine dispersion of organo-clay particles in the polymer matrix that provides large surface area for clay interacting with polymer matrix, which led to the restricted segmental motions near the organic-inorganic interfaces.^{21,22} At the rubbery plateau ($T = 150^\circ\text{C}$), an E' value of 61.3 MPa was measured for the nanocomposite, compared with 45.3 MPa for the virgin UV-cured polymer.

Thermogravimetric analysis thermograms of organoclay/polyurethane nanocomposites were shown in Figure 7. From the TGA data, it was clear that the decomposition onset and mid-point degradation temperature of the nanocomposite shifted toward the higher temperature with the increment of organoclay loading. After a complete decomposition, the residual mass of organoclay/polyurethane nanocomposite

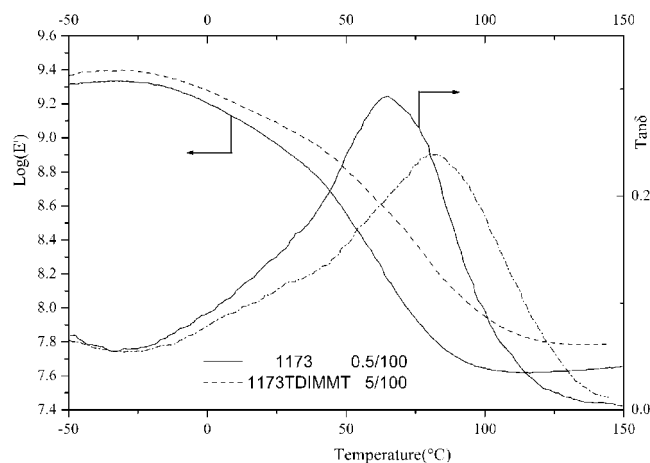


Figure 6 Influence of the clay filler on the elastic modulus and $\tan \delta$ profile recorded by DMA for a UV-cured polyurethane-acrylate.

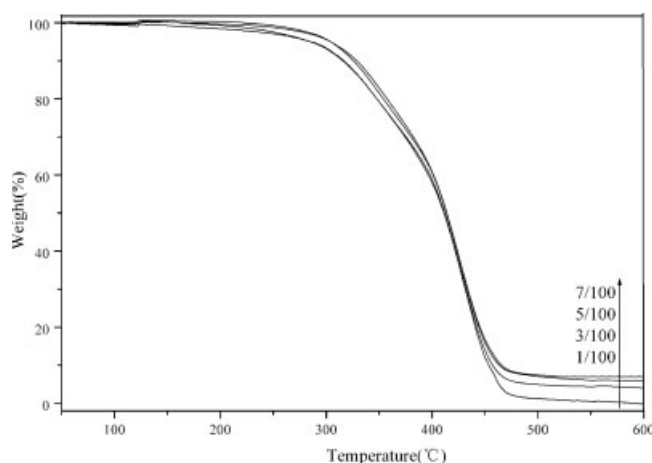


Figure 7 The TGA curves of organoclay/polyurethane nanocomposites.

were almost corresponding to the organoclay loading. This result showed that the exfoliated nanocomposites (Fig. 5) were more stable than the others, which might be attributed to maximized interaction between the clay and the polymer in an exfoliated nanocomposite structure due to the availability of larger surface area of clay for polymer matrix. This led to restricted thermal motions of the polymer molecules near the clay surface. On the other hand, higher decomposition temperatures of the organoclay/polyurethane nanocomposite may be ascribed to confinement of more polymer chains in between MMT layers.²³

The water sorption was also important for the mechanical properties in application in a humid environment or in outdoor applications. The major drawbacks of water sorption that have often been reported were its plasticizing effect, leading to a reduced glass transition temperature, decreased modulus and compressive strengths, chain scission and hardener degradation as well as possible detachment of the resin from the fiber in composite materials.^{24–25} In Figure 8,

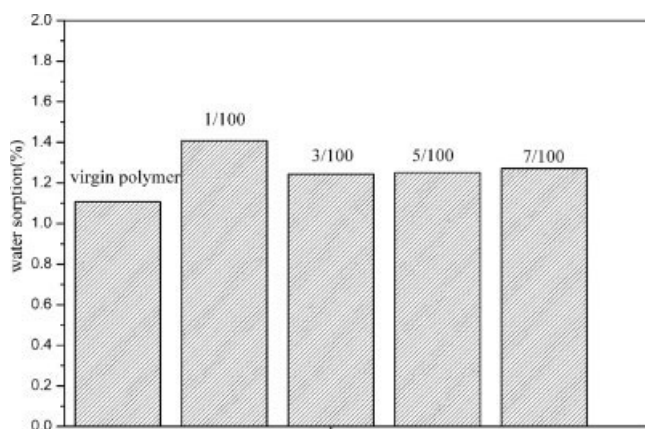


Figure 8 Water sorption of polymers with organoclays at various concentration.

the water sorption of clear polymer was just only 1.12%, however, when the organoclay was presented in the polymer, which caused a small increase of the water sorption, which was attributed to the hydrophilicity of 1173TDIMMT after UV photolysis.

CONCLUSIONS

A photoinitiator 1173TDI was synthesized, which was intercalated into montmorillonite through cationic exchange. The intercalated photoinitiator also had high photoinitiation efficiency, even only 1/100 (w/w) modified-clay could initiate the radical polymerization with the 87% acrylate conversion on 20 mW/cm² exposure. The d spacing could be enlarged to 13.9 nm after photopolymerization with 5/100 (w/w) organoclay loading. High thermal stability and high stiffness as well as homogeneous morphology were all possible even with only a little loading.

References

1. Decker, C. *Macromol Rapid Commun* 2002, 23, 1067.
2. Yang, X. M.; Lu, Y. *Mater Lett* 2005, 59, 2484.
3. Benfarhi, S.; Decker, C.; Keller, L.; Zahouily, K. *Eur Polym J* 2004, 40, 493.
4. Tyan, H. L.; Liu, Y. C.; Wei, K. H. *Chem Mater* 1999, 11, 1942.
5. Paul, D. R.; Zeng, Q. H.; Yu, A. B.; Lu, G. Q. *J Colloid Interface Sci* 2005, 292, 462.
6. Arroyo, M.; Machado, M. A. L.; Herrero, B. *Polymer* 2003, 44, 2447.
7. Songa, L.; Hua, Y.; Tang, Y.; Zhang, R.; Chena, Z.; Fan, W. *Polym Degrad Stab* 2005, 87, 111.
8. Hsu, S. L.; Wang, U.; King, J. S.; Jeng, J. L. *Polymer* 2003, 44, 5533.
9. Benfarhi, S.; Decker, C.; Keller, L.; Zahouily, K. *Eur Polym J* 2004, 40, 493.
10. Zahouily, K.; Benfarhi, S.; Bendaikha, T.; Baron, J.; Decker, C. *Proc Rad Tech Eur* 2001, 583.
11. Decker, C.; Keller, L.; Zahouily, K.; Benfarhi, S. *Polymer* 2005, 46, 6640.
12. Fawn, M. U.; Davuluri, S. P.; Wong, S. C.; Dean, C. *Webster Polym* 2004, 45, 6175.
13. Xu, G. C.; Li, A. Y.; Zhang, L. D.; Wu, G. S.; Yuan, X. Y.; Xie, T. *J Appl Polym Sci* 2003, 90, 837.
14. Keller, S. L.; Decker, C.; Zahouily, K.; Benfarhi, S. *Polymer* 2004, 45, 7437.
15. Uhl, F. M.; Davuluri, S. P.; Wong, S. C.; Webster, D. C. *Chem Mater* 2004, 16, 1135.
16. Weimer, M. W.; Chen, H.; Giannelis, E. P.; Sogah, D. Y. *J Am Chem Soc* 1999, 121, 1615.
17. Nese, A.; Sen, S.; Tasdelen, M. A.; Nugay, N.; Yagci, Y. *Macromol Chem Phys* 2006, 207, 820.
18. Brown, J. M.; Curliss, D.; Vaia, R. A. *Chem Mater* 2000, 12, 3376.
19. Lee, T. Y.; Bowman, C. N. *Polymer* 2006, 47, 6057.
20. Delozier, D. M.; Orwoll, R. A.; Cahoon, J. F.; Ladislav, J. S.; Smith, J. G. J.; Connell, J. W. *Polymer* 2003, 44, 2231.
21. Landry, C. J. T. *Macromolecules* 1993, 26, 3702.
22. Huang, H. H.; Order, B.; Willces, G. L. *Macromolecules* 1987, 20, 1322.
23. Blumstein, A. *J Polym Sci Part A: Gen Pap* 1965, 3, 2665.
24. Andreopoulos, A. G.; Tarantili, P. A. *J Appl Polym Sci* 1998, 70, 747.
25. Becker, O.; Varley, R. J.; Simon, G. P. *Eur Polym J* 2004, 40, 187.